

# Interpretation on Performance of Two Drilled Shafts Subjected to Tensile Loading Considering Concrete Cracking Effect

San-Shyan Lin<sup>1</sup>, Tai-Hong Chen<sup>1</sup> and Chia-Hong Lai<sup>1</sup>

<sup>1</sup>Department of Harbor and River Engineering, National Taiwan Ocean University, Keelung, Taiwan 20224  
Email:sslin46@gmail.com

**ABSTRACT:** In this paper, conversion of measured strain data into pile loads for tensile load testing of two drilled shafts is studied using the secant modulus of concrete. A back analysis method, considering the possible effect of concrete cracking or slippage between steel-grout interface, is used in converting the strain into pile loads. Subsequently, the t-z curves along shaft are obtained based on the pile loads interpreted from back analysis.

Keywords: drilled shaft, tensile loading test, back calculation, hyperbolic model

## 1. INTRODUCTION

Pile tensile load testing is used either to verify carrying capacity of the preliminary design or to determine ultimate frictional resistance of a pile foundation. In the latter case, strain gages are often installed at selected depth along the pile for measurement of strain distribution and subsequently converted into pile load. The conversion procedure requires the property of the axial stiffness of the tested pile. For tensile load testing, it is often carried out by holding the rebar cage on the pile top during testing. The testing results may be affected by the bond strength between concrete and steel interface. In the following, the pile refers to drilled shaft in this paper.

In this paper, two tensile load testing data are collected from local contractors in Taipei. The secant modulus of concrete versus strain and the stress-strain relationship of the concrete at uppermost installed gage level of all cases are derived first for comparison. A back analysis method using hyperbolic model is used in converting the strain into pile loads.

## 2. The Secant Modulus of Concrete

The secant modulus of concrete of the tested pile is often interpreted from collected strain data at the uppermost rebar gages installed near the pile head. In order to calculate the stress level in a drilled shaft, it is assumed that the measured strain from the gages are representative of the entire cross section (Lam and Jefferis 2011). In addition, it is also assumed that the modulus versus strain relationship at the uppermost gage level can be applied to the remainder of the pile. On more assumption of the method is that the frictional resistance between the soil and the pile from ground surface to the uppermost gage installed level is neglected under the given applied load at head. In this regard, the uppermost set of rebar gages need to be placed near the pile head to minimize the loss of the pile load due to shaft resistance. In the meantime, it also needs to consider the end effect or the Saint Venant principle (Lam and Jefferis 2011). In general, the rebar gage is installed at depth approximately equal to the width of the shaft. In Taiwan, most of the pile load testing installs the uppermost rebar gage at level of 1m to 3m below pile head (Lin et al. 2007). The second gage level is installed at the cut-off level. The procedures of computing the secant modulus of concrete are reviewed in the following:

The steel stress is given in the following equation

$$\sigma_s = E_s \epsilon_s \quad (1)$$

where  $E_s$  = elastic modulus of the steel and  $\epsilon_s$  = measured strain from the rebar strain gage. The steel force can be obtained by multiplication of the steel stress by the cross-sectional area of steel. Similarly, the concrete force is equal to the subtraction of the steel force from the applied force at the pile head.

Assuming stain compatibility, we have

$$\epsilon_s = \epsilon_c \quad (2)$$

Subsequently, the concrete modulus can be calculated as

$$E_c = \frac{P - F_s}{A_c \epsilon_s} \quad (3)$$

in which  $\sigma_c$  is the concrete stress. Multiplication of the concrete stress and the steel stress by the concrete area and the steel area, respectively, the pile load can be calculated by summing these two values as given in Eq. (4)

$$P = \sigma_c A_c + \sigma_s A_s \quad (4)$$

The resulting modulus values given in Eq. (3) are often plotted against strain, whose relationship is then modelled with a best fit curve such as exponential or polynomial equation. In case of using exponential equation, the stress-strain relationship can be expressed as

$$\sigma_c = E_c \epsilon_c \quad (5)$$

where  $E_c$  and  $\epsilon_c$  are constants. Under any rebar strain gage level, the pile axial force can be expressed as

$$P = \{ [E_c \epsilon_c] \times A_c + \sigma_s A_s \} \quad (6)$$

Once concrete cracked or slippage occurred at steel-grout interface under tensile load, the tensile stresses resulted from tensile load will gradually carry by the steel reinforcement only. Hence, the readout from the rebar strain gages will deviate from the assumption of stain compatibility in Eq. (2), because the strain in steel reinforcement is not equal to the strain in concrete.

## 3. Back Analysis Method

A hyperbolic model (Lin et al. 2007) is used to simulate the nonlinear behavior at the interface between pile shaft and surrounding soil. Beyond this nonlinear behavior at the interface, the shear stress versus displacement behavior of the soil field is modeled as linear behavior. A back analysis method (Xiao et al. 2003) is adopted to determine the required parameters based on the pile load test result.

The assumed shear stress and relative displacement relationship at the pile/soil interface is shown in Fig. 1 can be approximated by a hyperbolic equation having the form of:

$$\tau = \frac{\Delta}{1 + \Delta} \quad (7)$$

Based on the instrumented rebar strain gage readout during the pile load test, the pile load distribution along depth can be calculated. Subsequently, an spline interpolation function can be applied to fit the measured data to obtain a load distribution along depth function, which can then be used to determine the shear stresses along depth at each loading stage using the following equation:

$$= -\frac{1}{2} \frac{P_i(z)}{P_0} \quad (8)$$

in which  $P_i(z)$  is the Spline fitted function. The value of  $b$  at various depth can be calculated as  $b = \frac{P_i(z)}{P_0}$ , in which is in general between 0.85 and 0.95.

The displacement at any depth of it's corresponding loading step is calculated using the following equation:

$$= -\frac{1}{2} \int_0^z P_i(z) \quad (9)$$

in which  $E$  and  $A$  are the elastic modulus and the cross-sectional area of the pile, respectively. The value of  $b$  at various depth can be obtained using the following equation:

$$b = \frac{(1 - \nu)(1 - \nu)}{(1 - \nu)(1 - \nu)} \quad (10)$$

The initial shear stiffness of pile/soil interface is

$$= 1/b \quad (11)$$

#### 4. Case Studies

The basic information on six collected tensile load testing is given in Table 1. These two piles were installed by reverse circulation method. The ground conditions of the D1 and D3 sites are given in Table 2 and 3, respectively. The nonlinear stress- strain relationship of the concrete of the case examples at the uppermost gage level is shown in Fig. 2.

In order to determine  $a$  and  $b$  parameters given in Fig. 1, the pile axial load along depth at each corresponding loading steps is calculated first as shown in Fig. 3 and 4 for D1 and D3 piles, respectively. However, the calculated pile axial force becomes unreasonably high at some gage levels when the applied loading becomes higher, as shown in these figures. The reasons for such a high axial load at these gages are most possibly affected by the bond strength between concrete and steel interface, which may have caused slippage between mortar and steel interface or even caused concrete cracking. Hence, the assumption of strain compatibility in Eq. (2) does not apply. The measured strain becomes taken by the steel only instead of taking by both steel and concrete. It's the possible reasonable to have such a high axial force at certain gage levels.

An interpolation spline function is used to fit the measured data to obtain a load distribution with depth shown in Figs. 3 and 4 for piles D1 and D3, respectively. The interpolation is based on the gage readouts of the uppermost, the second set and the bottom gages for the fitting. The axial load versus displacement relationships of both piles is shown in Fig. 5.

Figures 6 and 7 show the results of the calculated initial stiffness and ultimate strength at the pile/soil interface along shaft. The  $t$ - $z$  curves close to the pile head and close to the pile toe are shown in Fig. 8 and 9, respectively.

Table.1 Tested pile information

Pile	Loading Method	Diameter	Depth	Construction Method
D1	Tensile	1.5m	45.7m	Reverse circulation method
D3	Tensile	1.5m	49.7m	Casing method

Table.2 Subsurface condition at D1 site

Depth	Desc-ription	Class-ificati-on	SPT N	Unit weight (kN/m <sup>3</sup> )	C (kN/m <sup>2</sup> )
0.0~2.8	Backfill	SF	1.5~2	-	-
2.8~3.5	Very soft silty clay	CL	1.5	17.84	20.6
3.5~15.45	Very soft silty clay	CL	1~1.5	17.37	24.5
15.45~18.5	Soft silty clay	CL	2.5~3	17.47	36.3
18.5~22.0	Soft silty clay and some sand	CL	3~4.5	17.69	39.2
22.0~23.85	Silty sand	SM	9	-	-
23.85~38.6	Andesite rock, gravel and silty sand mixture	-	20 ~ 50/8cm	-	-
38.6~39.3	Sandstone	-	50/5cm	-	-
39.3~44.0	Sandstone /Shale	-	50/3cm	-	-

Table.3 Subsurface condition at D3 site

Depth	Desc-ription	Class-ificati-on	SPT N	Unit weight (kN/m <sup>3</sup> )	C (kN/m <sup>2</sup> )
0.0~2.5	Backfill	SF	11	-	-
2.5~4.5	Firm silty clay	CL	4~5	-	-
4.5~13.0	Very soft silty clay	CL	1~1.5	17.63	45.1
13.0~25.5	Soft silty clay	CL	2~4	17.38	33.4
25.5~37.5	Firm silty clay	CL	5~8	17.53	43.2
37.5~41.7	Stiff silty sand	ML	10~14	19.04-	76.5
41.7~43.0	Silty sand	-	14	-	-
43.0~70.5	Andesite rock and some silty sand	-	50/13cm ~ 50/6cm	-	-

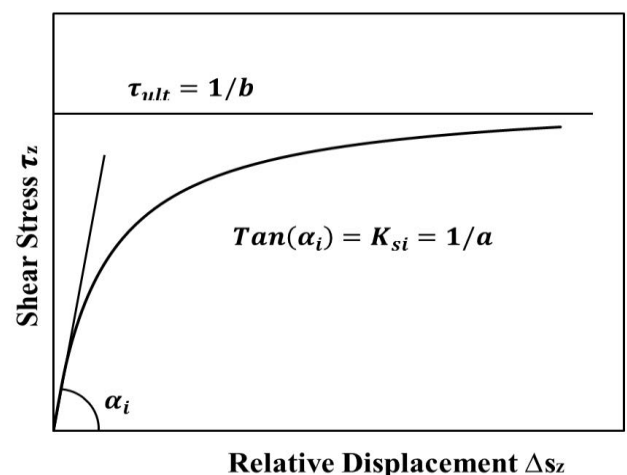


Fig.1 Assumed shear stress vs relative displacement at the pile/soil interface

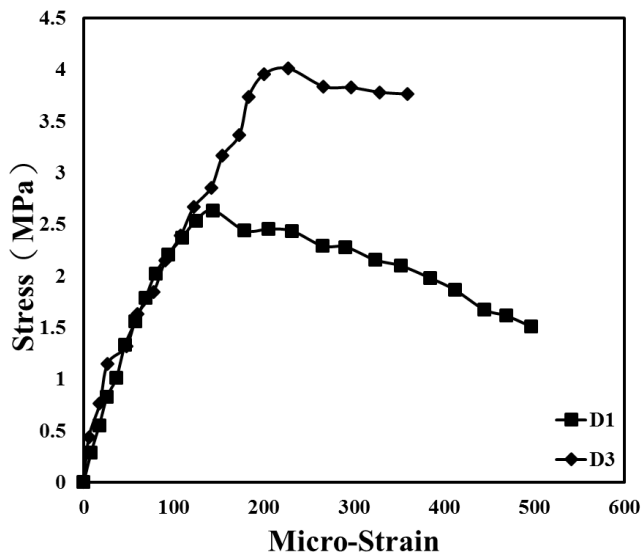


Fig.2 Concrete stress-strain relationship

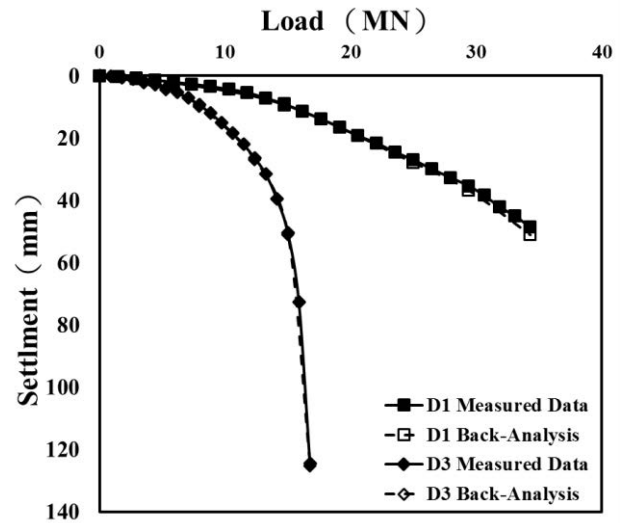


Fig. 5 Load vs displacement relationship at pile head

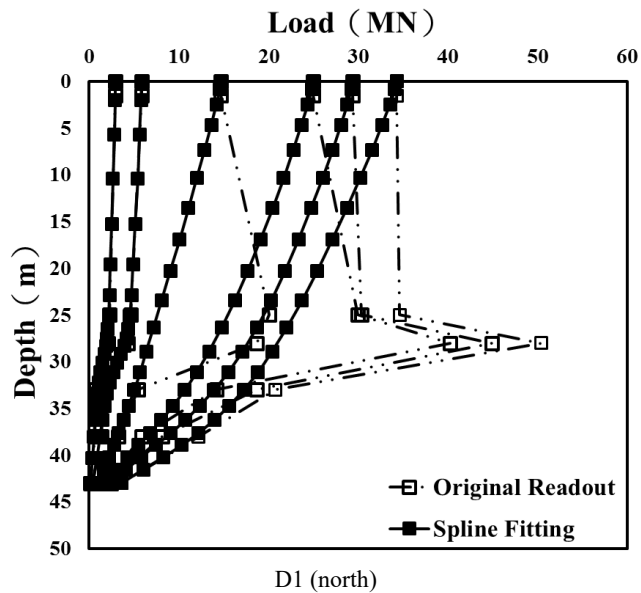


Fig. 3 Axial load along shaft of D1 pile

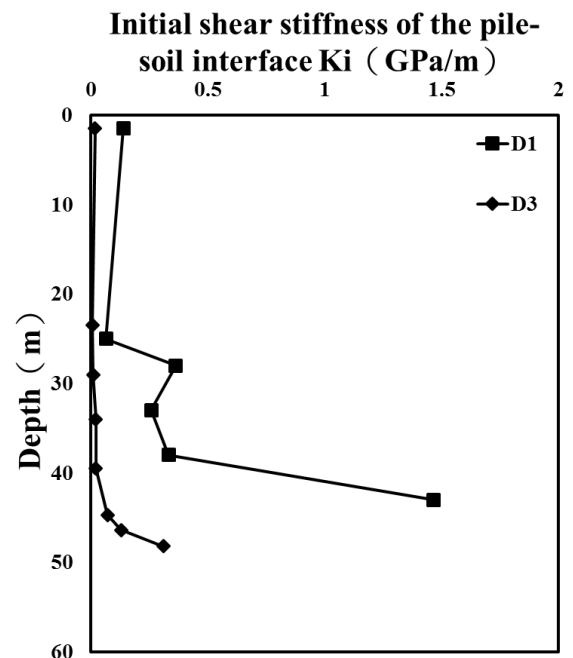


Fig. 6 Predicted  $K_{si}$  profile

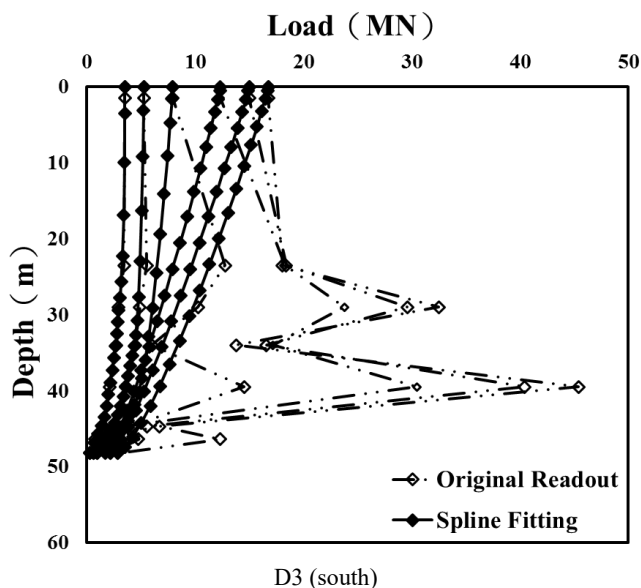


Fig. 4 Axial load along dept of D3 pile

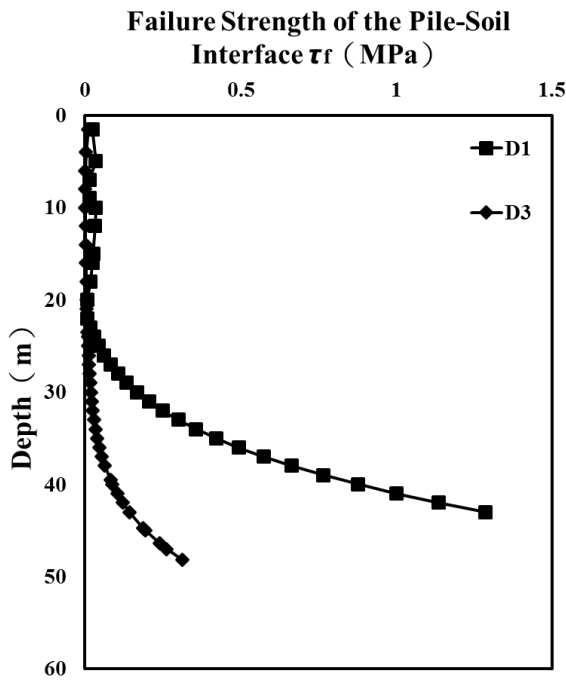


Fig. 7 Predicted  $\tau_f$  profile

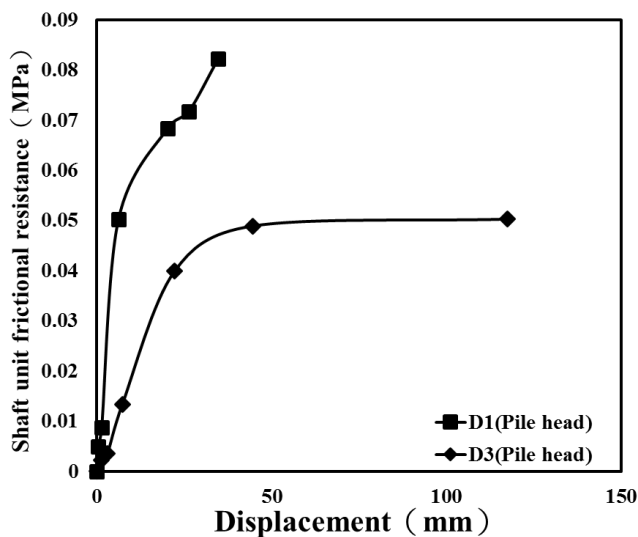


Fig. 8 Interpreted t-z curves close to pile head

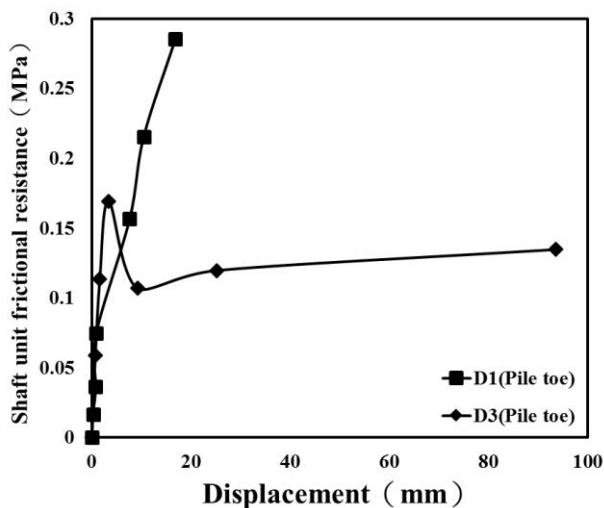


Fig. 9 Interpreted t-z curves close to pile toe

## 5. Conclusions

Back analysis method was used in this paper to interpret the required parameters based on tensile loading tests of two drilled shafts. More reasonable axial force along pile shaft was fitted using hyperbolic model. Subsequently, the t-z curves along shaft are obtained based on the pile loads interpreted from back analysis.

Based on the back calculation of these two tested piles, the following conclusions can be drawn:

- The initial shear stiffness at soil/pile interface  $K_{si}$  of D1 was higher than that of D3.
- The failure strength  $\tau_f$  of D1 was also higher than that of D3 especially at depth 22m below ground surface.
- Based on the t-z curves given in Figs. 8 and 9, the D1 pile was not yet reached the ultimate value. However, hardening and softening behavior was observed for the D3 pile close to head and close to toe, respectively.

## 6. Acknowledgement

The present study was carried out as part of a research project funded by Ministry of Science and Technology (NSC 102-2221-E-019-028-MY3), Taiwan. The author is grateful for the financial support.

## 7. References

- Lam, C. and Jefferis, S.A., (2011) "Critical Assessment of Pile Modulus Determination Methods," *Canadian Geotechnical Journal*, Vol. 48, No. 10, 1433-1448.
- Lin, S.S., Wang, K.J., Hsieh, H.S., Chang, Y.H., and Huang, C.S., (2007) "Field Testing of Axially Loaded Drilled Shafts in Clay/Gravel Layer," *Journal of GeoEngineering*, Vol. 2, No. 3, 123-128.
- Xiao, Z. R. Du, M.F., and Zhang, Z (2003) "A Back Analysis Method to Determine the Parameters for the Pile Foundation Analysis in Foundation: Innovations, Observations", *Design and Practice*, Thomas Telford, London, UK, pp.951-960.